Original Article

Renal R2* as a noninvasive predictor of hepatorenal syndrome-acute kidney disease in cirrhotic patients with ascites: a retrospective cohort study

Jae Hyon Park[1,2]^, Hee Jun Park[2]^, Daeun Choi[2]^, Jongjin Yoon[2]^

[1]Department of Radiology, Armed Forces Daejeon Hospital, Daejeon, Korea; [2]Department of Radiology and Research Institute of Radiological Science, Severance Hospital, Yonsei University College of Medicine, Seoul, Korea

Contributions: (I) Conception and design: JH Park; (II) Administrative support: J Yoon; (III) Provision of study materials or patients: JH Park, HJ Park, D Choi; (IV) Collection and assembly of data: HJ Park, D Choi, J Yoon; (V) Data analysis and interpretation: JH Park, J Yoon; (VI) Manuscript writing: All authors; (VII) Final approval of manuscript: All authors.

Correspondence to: Jongjin Yoon, MD, PhD. Department of Radiology and Research Institute of Radiological Science, Severance Hospital, Yonsei University College of Medicine, 50-1 Yonsei-ro, Seodaemun-gu, Seoul, 03722, Korea. Email: jayzin@yuhs.ac.

Background: Hepatorenal syndrome-acute kidney disease (HRS-AKD) is associated with poor renal outcomes in cirrhotic patients, yet no established noninvasive imaging marker exists for its early prediction. This study evaluated renal R2* derived from magnetic resonance elastography (MRE) with multi-echo R2* mapping as a noninvasive imaging marker for predicting the development of HRS-AKD in cirrhotic patients with ascites.

Methods: This retrospective observational study analyzed 376 patients who underwent liver MRE with multi-echo R2* mapping between January 2018 and October 2024. Median renal R2* values were quantified from the left kidney using radiomics-based analysis. HRS-AKD was defined as an estimated glomerular filtration rate (eGFR) <60 mL/min/1.73 m^2 or a ≥50% increase in serum creatinine from baseline within 3 months after MRE, without other causes of renal disease. Diagnostic performance of renal R2* was compared with liver stiffness and serum fibrosis markers, including the aspartate aminotransferase-to-alanine aminotransferase ratio (AAR), aspartate aminotransferase-to-platelet ratio index (APRI), and fibrosis-4 (FIB-4) index. Multivariable logistic regression identified independent predictors of HRS-AKD.

Results: Among cirrhotic patients with ascites, 12.9% developed HRS-AKD; 62.5% had a prior episode of HRS-acute kidney injury (AKI). Median renal R2* was higher in patients who developed HRS-AKD (P=0.007), and inversely correlated with eGFR measured at MRE (r=–0.34, P=0.006). Renal R2* did not correlate with serum iron markers or hemoglobin (all P≥0.05). The area under the receiver operating characteristic curve (AUROC) of renal R2* was 74.5 [95% confidence interval (CI): 57.4–91.6] for predicting HRS-AKD, outperforming liver stiffness and serum fibrosis markers. An R2* cut-off of 20.8 s^{-1} yielded 75% sensitivity and 74% specificity. R2* ≥20.8 s^{-1} was an independent predictor of HRS-AKD [odds ratio (OR) 16.8; P=0.002].

Conclusions: Renal R2* is a promising noninvasive imaging marker candidate for predicting the development of HRS-AKD in cirrhotic patients with ascites.

Keywords: Elasticity imaging technique; hepatorenal syndrome; liver cirrhosis; magnetic resonance imaging (MRI); renal insufficiency

Submitted Oct 29, 2025. Accepted for publication Mar 27, 2026. Published online May 19, 2026.
doi: 10.21037/qims-2025-aw-2262
View this article at: https://dx.doi.org/10.21037/qims-2025-aw-2262

^ ORCID: Jae Hyon Park, 0000-0002-7626-194X; Hee Jun Park, 0009-0006-6829-6196; Daeun Choi, 0000-0001-9741-926X; Jongjin Yoon, 0000-0003-4733-7658.

Introduction

Hepatorenal syndrome-acute kidney disease (HRS-AKD) is a form of kidney dysfunction in cirrhotic patients, defined by reduced renal function in the absence of other identifiable causes (1). It represents a transitional stage between acute kidney injury (AKI) and chronic kidney disease (CKD), and is associated with higher rates of CKD progression and mortality compared to HRS-AKI (2-4). Although often preceded by HRS-AKI, HRS-AKD can also occur *de novo* and independently increase the risk of long-term renal dysfunction, even without a preceding HRS-AKI (4), underscoring the need for early detection during the subacute "window period" when intervention may still alter outcomes.

The pathophysiology of HRS-AKD involves sustained renal vasoconstriction triggered by systemic and splanchnic vasodilation, leading to renal hypoperfusion and persistent renal hypoxia (5). This process is often exacerbated by complications such as spontaneous bacterial peritonitis, variceal bleeding, or large-volume paracentesis without adequate albumin (6). Historically classified as type 1 or type 2 HRS, renal dysfunction in cirrhosis is now categorized as HRS-AKI, HRS-AKD, or HRS-CKD based on the timing and duration of kidney injury (1). According to current criteria, AKD in cirrhosis is defined as an estimated glomerular filtration rate (eGFR) <60 mL/min/1.73 m^2 for less than 3 months, or a serum creatinine increase of greater than50% from baseline within the same time frame (7). The incidence of AKD in cirrhotic patients has been reported to reach up to 30%, with risk factors including advanced age, diabetes, preexisting CKD, stage 2 or 3 AKI, ascites, and bacterial infections (4).

Despite its clinical relevance, no prior study has focused on identifying noninvasive imaging markers for HRS-AKD. Most existing research has concentrated on HRS-AKI biomarkers, such as plasma cystatin C, urine neutrophil gelatinase-associated lipocalin (NGAL), and urine interleukin-18 (IL-18) (8-10). These markers reflect acute tubular injury and may not adequately capture the subacute AKI-to-CKD transition typical of HRS-AKD, highlighting the need for novel diagnostic tools.

Therefore, this study evaluated candidate imaging marker for HRS-AKD in patients with cirrhosis, focusing on renal R2* quantification using magnetic resonance elastography (MRE) with multi-echo R2* mapping as a noninvasive imaging biomarker. We present this article in accordance with the STROBE reporting checklist (available at https://qims.amegroups.com/article/view/10.21037/qims-2025-aw-2262/rc).

Methods

Study patients

This retrospective observational cohort study was conducted in accordance with the Declaration of Helsinki and its subsequent amendments. The study was approved by the Institutional Review Board (IRB) of Severance Hospital, Seoul, Korea (IRB No. 2025-0959-001). The requirement for informed consent was waived due to the retrospective nature of the study. While MRE is not routinely performed in cirrhotic patients, it is routinely obtained at our institution for liver transplant candidates to assess liver stiffness, portal hypertension and parenchymal iron or fat content. Using electronic medical records, 561 patients who underwent MRE with multi-echo R2* mapping (hereafter referred to as MRE) from January 2018 to October 2024 were identified. The exclusion criteria were as follows: (I) patients who had undergone partial or complete nephrectomy of the left kidney, or whose left kidney was not fully included in the scan field; (II) cases where the margin of the left kidney could not be confidently identified during segmentation; (III) poor-quality MRE images or those with obvious artifacts; (IV) absence of pre-MRE laboratory results within one week of the MRE; and (V) kidney damage due to other causes. Based on these exclusion criteria, a total of 376 patients were analyzed (*Figure 1*).

Clinical and demographic data were extracted, including age, sex, body mass index (BMI), comorbidities (hypertension, type 2 diabetes mellitus, coronary artery occlusive disease), underlying liver disease, and pre-MRE laboratory results. For patients with cirrhosis and ascites, the incidence of HRS-AKI within one week prior to the date of liver MRE was also recorded. HRS-AKI was defined as an absolute increase in serum creatinine ≥0.3 mg/dL within 48 hours and/or ≥50% increase from the most recent outpatient serum creatinine value within the past 3 months, used as the baseline (1,11). The presence and severity of ascites, along with hepatocellular carcinoma, were assessed on the same magnetic resonance imaging (MRI) used for MRE by a board-certified radiologist. Ascites severity was categorized as none, mild, or moderate-to-severe, following the grading criteria established by the International Ascites Club and the European Association for the Study of the Liver (EASL) guidelines for decompensated cirrhosis (12,13).

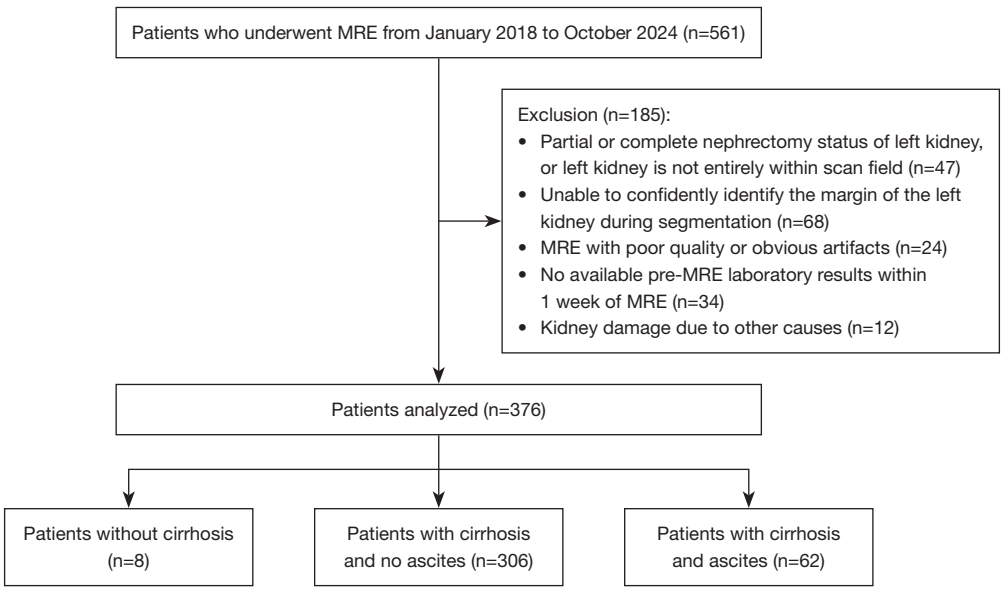

Figure 1 Flowchart illustrating patient selection for the study. MRE, magnetic resonance elastography.

Mild ascites was defined as trace fluid without abdominal distension, while moderate ascites indicated visible fluid accumulation with moderate to marked distension. Additionally, iron overload was defined as ferritin >200 μg/L and transferrin saturation >45% in women, and ferritin >300 μg/L and transferrin saturation >50% in men (14).

MRE

All patients underwent liver MRE using a 3.0-T MRI scanner (Discovery mR750W, GE Medical Systems, Milwaukee, WI, USA) equipped with 32-channel torso coil. A 19-cm diameter passive pneumatic driver was placed over the right rib cage and was connected to a waveform generator via a pneumatic tube. A 60-Hz acoustic wave was transmitted to the driver to induce liver vibrations. Four trans-axial slices were obtained with a 14s-breath hold. Wave images and elastogram images (stiffness map) with cross-hatching marks were automatically generated on the operating console. Cross-hatching marks represented the 95% confidence threshold mask, indicating areas unsuitable for stiffness measurement. The imaging parameters for spin-echo echo-planar image MRE were as follows: repetition time (TR), 1,000 ms; echo time (TE), 62 ms; matrix size, 64×64; slice thickness 8 mm; and flip angle, 90°. For T2-weighted imaging, the parameters were: TR, 540 ms; TE, 80 ms; matrix size, 320×256; slice thickness, 8 mm; and flip angle, 90°. For R2* mapping, the parameters were: TR, 7.24 ms; TE, minimum full (0.9–4.4 ms); number of echoes, 6; matrix size, 160×128; slice thickness, 6 mm; and flip angle, 4°. R2* mapping was obtained during a single breath-hold (<17 s) using commercially available chemical shift-encoded pulse sequence (IDEAL IQ; GE Healthcare, Milwaukee, WI, USA), which automatically corrects for fat-water signal interference. To minimize motion artifacts, acquisitions were performed at end-expiration, and cases with severe respiratory or ascites-related motion were excluded after visual quality assessment.

Liver stiffness quantification

Liver stiffness was measured by a board-certified radiologist with 5 years of experience in abdominal radiology by placing the largest possible freehand regions of interests (ROIs) on the stiffness map, primarily within the right hepatic lobe. Areas with apparent pathological lesions, large vessels, inadequate wave propagation (e.g., hot spots or dark spots), and cross-hatching artifacts were carefully avoided. At least four ROIs were obtained for each patient, and the mean ROI was used for the analysis.

Median renal R2 quantification*

Two board-certified radiologists, each with 5 years of experience in genitourinary radiology, independently segmented the left kidney on R2* maps using 3D Slicer

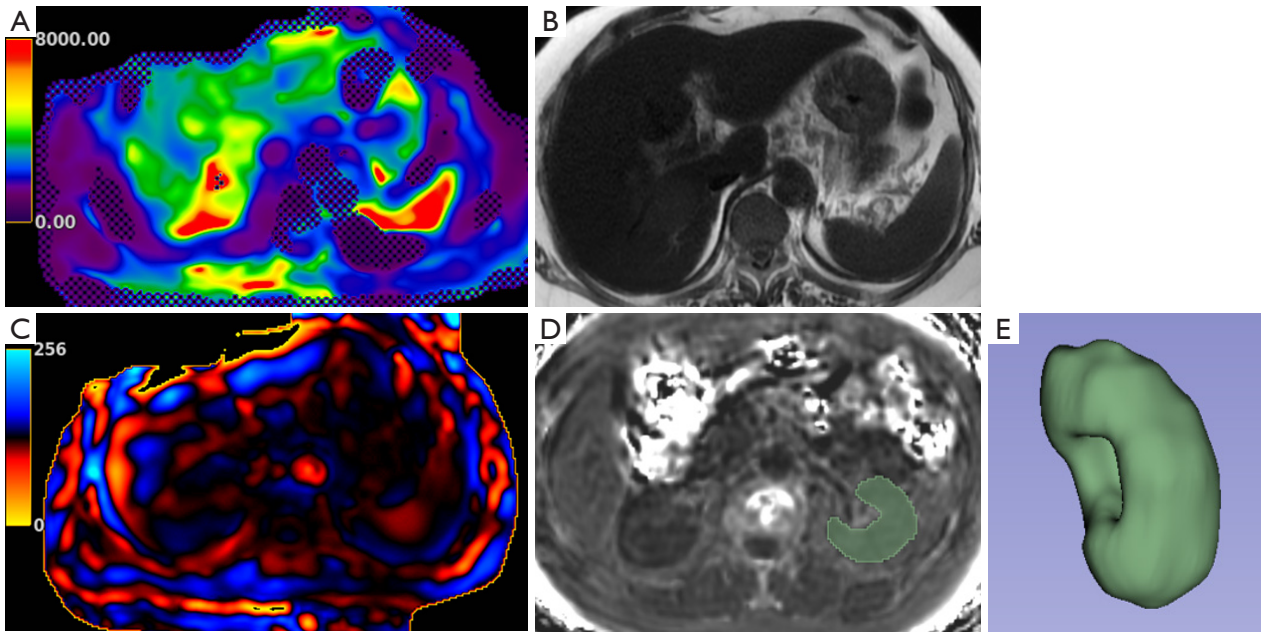

Figure 2 MRE in a 69-year-old male patient. (A) Color-coded liver elastogram with 95% confidence overlay, (B) axial T2-weighted image, (C) shear wave image, (D) axial R2* map with segmented left kidney (green), and (E) 3D rendering of the segmented left kidney. Liver stiffness measured 3.4 kPa on MRE. 3D, three-dimensional; MRE, magnetic resonance elastography.

version 4.10 (www.slicer.org), a free and open-source software. During segmentation, care was taken to avoid areas potentially affected by artifacts, including contamination with renal sinus or perirenal fat, and benign renal lesions (*Figure 2*). All segmentation masks were independently reviewed and confirmed by another board-certified genitourinary radiologist, with discrepancies resolved by consensus. First order median values of the masks were extracted using Pyradiomics, an open-source Python package (version 2.2.1; https://pyradiomics.readthedocs.io), via radiomics.featureextractor.RadiomicsFeatureExtractor class. The following settings were applied: 'binWidth': 20, 'resampledPixelSpacing': [3, 3, 3], 'interpolator': sitk.sitkBSpline, 'normalize': False, 'normalizeScale': 1, 'removeOutliers': False, and 'sigma': [–3, 3]. Normalization was not applied, as R2* values are directly measured from the R2* map by selecting a region of interest in clinical practice.

Serum fibrosis markers

The aspartate aminotransferase (AST)/alanine aminotransferase (ALT) ratio (AAR), the AST-to-platelet ratio index (APRI), and the fibrosis-4 (FIB-4) index were calculated using the following formulas, where ULN refers to the upper limit of the normal AST, and PLT denotes the platelet count:

$$\text{AAR} = \frac{\text{AST}(\text{IU/L})}{\text{ALT}(\text{IU/L})} \quad [1]$$

$$\text{APRI} = \frac{\text{AST}(\text{IU/L})}{\text{ULN AST}/\text{PLT}(10^9/\text{L})} \times 100\% \quad [2]$$

$$\text{FIB-4 index} = \frac{\text{Age}(\text{years}) \times \text{AST}(\text{IU/L})}{\text{PLT}(10^9/\text{L}) \times \text{ALT}(\text{IU/L})^{1/2}} \quad [3]$$

Study outcomes and definitions

The primary outcome was diagnostic accuracy of median renal R2* for predicting the development of HRS-AKD in patients with cirrhosis and ascites within 3 months after the date of liver MRE. This accuracy was compared with that of MRE and serum fibrosis markers, including AAR, APRI, and FIB-4 index. Specifically, HRS-AKD was defined as an eGFR <60 mL/min/1.73 m^2 in the absence of other identifiable causes of kidney disease, or a ≥50% increase in serum creatinine from baseline (1,11). Baseline was defined as the most recent stable serum creatinine value within 3 months prior to the date of liver MRE (1). When no prior

serum creatinine value was available within 3 months, the first documented serum creatinine value on the day of MRE was used as baseline. The eGFR was calculated using the 2021 Chronic Kidney Disease Epidemiology Collaboration (CKD-EPI) equation based on serum creatinine, age, and sex, wherein k=0.7 for women, and 0.9 for men; α=–0.241 for women, and –0.302 for men:

$$\text{eGFR} = 142 \times \min\left(\frac{Scr}{k},1\right)^{\alpha} \times \max\left(\frac{Scr}{k},1\right)^{-1.200} \times 0.9938^{age} \times \left[1.012 \text{ if woman}\right] \quad [4]$$

Secondary outcomes included the correlation between median renal R2* values and iron-related parameters and eGFR measured at the time of MRE, as well as the incidence of HRS-CKD, defined as eGFR <60 mL/min/1.73 m^2 for ≥3 months in the absence of other identifiable causes of kidney disease (1,11).

Statistical analysis

Continuous variables were analyzed using the student's t-test or the Mann-Whitney U-test after assessing the normality with the Shapiro-Wilk test. Categorical variables were evaluated using the Chi-squared test unless more than 20% of cells had expected frequencies below 5, in which case Fisher's exact test was applied. Correlations between median renal R2* and serum iron, ferritin, hemoglobin, and transferrin saturation were assessed using Spearman's rank correlation coefficient. Inter-reader agreement for R2* measurements was evaluated using intraclass correlation coefficient (ICC), and Bland-Altman analysis was performed to assess bias and limits of agreements between readers. ICC value was interpreted as follows: <0.50, poor; 0.5–0.75, moderate; >0.75–0.90, good; and >0.90 excellent reliability. Receiver operating characteristic (ROC) curves were generated, and the optimal cut-off value for median renal R2* to differentiate cirrhotic patients with ascites with and without HRS-AKD was determined. The optimal cut-off for each parameter was defined as the point on the ROC curve closest to 100% sensitivity and specificity. Univariable and multivariable Firth's penalized logistic regression analyses were performed to identify factors independently associated with HRS-AKD. A sensitivity analysis was conducted by adjusting for baseline renal function and by stratifying patients according to eGFR (≥60 *vs.* <60 mL/min/1.73 m^2) to evaluate the robustness of the association between renal R2* and HRS-AKD. All statistical analyses were performed using PRISM 6.0 software (GraphPad Software, Inc., San Diego, CA, USA), and Python 3.10.4 (Python Software Foundation). A two-tailed P value <0.05 was considered statistically significant.

Results

Baseline characteristics

The characteristics of the three patient groups are summarized in *Table 1*. Among patients with cirrhosis, 54.9% had underlying chronic hepatitis B infection. A significant increasing trend was observed in total bilirubin (P<0.001), hepatic encephalopathy (P<0.001), Child-Pugh score (P<0.001), and Model for End-Stage Liver Disease (MELD) score (P=0.001). Conversely, a significant decreasing trend was noted in platelet count (P<0.001). These trends were observed across the clinical spectrum from non-cirrhotic patients to cirrhotic patients without ascites, and finally to cirrhotic patients with ascites. Among the serum fibrosis markers, the AAR did not differ significantly among the three groups (P=0.55), whereas both the APRI and the FIB-4 index showed a significant increasing trend across the patient spectrum (P=0.023 for APRI, and P=0.042 for FIB-4 index). Among patients with cirrhosis and ascites, 16 (25.8%) patients experienced HRS-AKI within one week prior to the date of liver MRE, and 8 (12.9%) patients developed HRS-AKD within 3 months after MRE. Of these, 5 (62.5%) had a preceding episode of HRS-AKI.

Liver stiffness and median renal R2 values in patients with or without cirrhosis and ascites*

The median liver stiffness values measured by MRE showed a significant increasing trend from non-cirrhotic patients, to cirrhotic patients without ascites, and finally to cirrhotic patients with ascites (all P<0.05; *Figure 3*). In contrast, there were no significant differences in median renal R2* values among the three groups (all P≥0.05). The ICC of median renal R2* values was 0.86, indicating good inter-reader agreement. The Bland-Altman plot demonstrating the agreement between the two readers is presented in Figure S1.

In patients with cirrhosis, median liver stiffness values increased with the severity of ascites. However, a statistically significant difference was observed only between those without ascites and those with moderate ascites (P=0.026). Median renal R2* values did not differ significantly among cirrhotic patients with no ascites, mild ascites, or moderate ascites.

Table 1 Baseline characteristics of patients who underwent MRE (n=376)

Variable	Patients without cirrhosis (n=8)	Patients with cirrhosis and no ascites (n=306)	Patients with cirrhosis and ascites (n=62)	P value
Age (years)	59 (51.6–63.0)	59.0 (52.0–65.0)	58.5 (51.0–63.0)	0.82
Male	5 (62.5)	215 (70.3)	45 (72.6)	0.83
BMI (kg/m^2)	23.5 (22.1–25.4)	24.6 (22.2–27.4)	24.1 (22.3–26.2)	0.32
Hypertension	0 (0)	79 (25.8)	15 (24.2)	0.25
Type 2 DM	0 (0)	28 (9.2)	7 (11.3)	0.57
CAOD	0 (0)	10 (3.3)	3 (4.8)	0.71
Underlying liver disease				<0.001
Alcoholic	0 (0)	45 (14.7)	9 (14.5)	
Autoimmune	0 (0)	6 (2.0)	0 (0)	
Cardiac	0 (0)	1 (0.3)	0 (0)	
HBV	0 (0)	171 (55.9)	31 (50.0)	
HCV	0 (0)	12 (3.9)	8 (12.9)	
NASH	0 (0)	47 (15.4)	8 (12.9)	
PBC	0 (0)	2 (0.7)	1 (1.6)	
PSC	0 (0)	1 (0.3)	1 (1.6)	
Wilson	0 (0)	1 (0.3)	0 (0)	
Others	8 (100.0)	20 (6.5)	4 (6.5)	
Albumin (g/dL)	4.0 (3.8–4.4)	4.2 (3.5–4.5)	4.0 (2.9–4.5)	0.35
PT (INR)	1.0 (1.0–1.1)	1.0 (1.0–1.1)	1.1 (1.0–1.3)	0.16
AST (IU/L)	31.5 (26.0–49.5)	33.0 (25.0–44.0)	37.0 (28.0–59.0)	0.13
ALT (IU/L)	22.0 (17.5–36.5)	25.0 (17.0–37.8)	26.5 (16.0–42.8)	0.75
γ-GT (IU/L)	71.0 (59.0–144.0)	46.0 (28.0–89.0)	51.5 (25.5–102.5)	0.36
Total bilirubin (mg/dL)	0.5 (0.3–0.6)	0.9 (0.6–1.4)	1.3 (0.7–2.1)	<0.001
Hemoglobin (g/dL)	10.8 (9.6–11.6)	13.8 (11.3–14.8)	12.9 (10.0–14.8)	0.045
WBC count (10^3/μL)	4.5 (3.6–5.9)	5.1 (3.7–6.6)	4.6 (3.8–6.1)	0.44
Platelet count (10^3/μL)	168.5 (133.5–199.0)	136.0 (81.0–199.0)	120.5 (67.0–175.5)	0.042
CRP (mg/L)	4.1 (2.1–4.8)	2.1 (0.8–6.2)	2.1 (0.8–10.9)	0.61
Ferritin (ng/mL)	40.3 (26.3–161.0)	121.8 (54.8–250.1)	144.8 (50.1–358.2)	0.42
Iron (μg/dL)	60.0 (36.5–105.5)	91.5 (59.0–136.0)	76.0 (49.0–123.0)	0.43
Encephalopathy	0 (0)	15 (4.9)	11 (17.7)	0.001
Ascites				<0.001
Mild	6 (75.0)	0 (0)	35 (56.5)	
Moderate	2 (25.0)	0 (0)	27 (43.5)	
APRI	0.5 (0.4–0.6)	0.7 (0.4–1.2)	1.0 (0.5–1.8)	0.023

Table 1 *(continued)*

Table 1 *(continued)*

Variable	Patients without cirrhosis (n=8)	Patients with cirrhosis and no ascites (n=306)	Patients with cirrhosis and ascites (n=62)	P value
AAR	1.3 (1.2–1.5)	1.3 (0.9–2.1)	1.5 (0.9–2.4)	0.55
Fibrosis-4 index	2.2 (2.0–2.5)	2.9 (1.6–5.6)	4.1 (2.0–7.4)	0.042
CP score	5.0 (5.0–6.0)	5.0 (5.0–6.0)	7.0 (6.0–9.0)	<0.001
MELD score	6.0 (6.0–7.0)	7.0 (6.0–9.0)	9.0 (7.0–12.0)	0.001
HCC	0 (0)	175 (57.2)	34 (54.8)	<0.001
BUN (mg/dL)	17.3 (14.3–17.7)	14.6 (12.1–18.1)	14.3 (11.6–17.4)	0.66
Creatinine (mg/dL)	0.7 (0.6–0.8)	0.8 (0.7–1.0)	0.8 (0.7–1.0)	0.38
eGFR (mL/min/1.73 m^2)	102.0 (94.6–107.5)	100.3 (90.7–107.8)	100.8 (88.5–109.8)	0.93
HRS-AKI	–	–	16 (25.8)	–
HRS-AKD	–	–	8 (12.9)	–

Data are presented as number (percentage) or median (25^{th}–75^{th} percentile). HRS-AKI and HRS-AKD were assessed only for patients with cirrhosis and ascites. AAR, aspartate aminotransferase-to-alanine aminotransferase ratio; ALT, alanine aminotransferase; APRI, aspartate aminotransferase-to-platelet ratio index; AST, aspartate aminotransferase; BMI, body mass index; BUN, blood urea nitrogen; CAOD, coronary artery occlusive disease; CP, Child-Pugh; CRP, C-reactive protein; DM, diabetes mellitus; eGFR, estimated glomerular filtration rate; HBV, hepatitis B virus; HCC, hepatocellular carcinoma; HCV, hepatitis C virus; HRS-AKI, hepatorenal syndrome acute kidney injury; HRS-AKD, hepatorenal syndrome acute kidney disease; INR, international normalized ratio; MELD, Model for End-Stage Liver Disease; MRE, magnetic resonance elastography; NASH, non-alcoholic steatohepatitis; PBC, primary biliary cholangitis; PSC, primary sclerosing cholangitis; PT, prothrombin time; WBC, white blood cell count; γ-GT, gamma-glutamyl transferase.

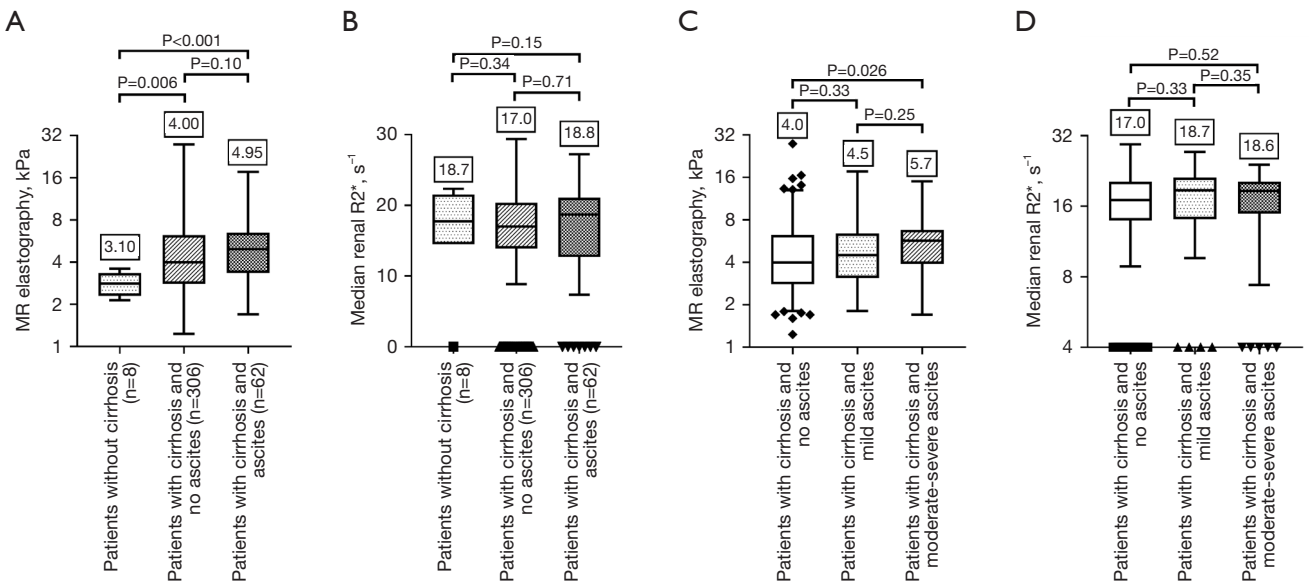

Figure 3 Comparison of liver stiffness and renal R2* across patient groups stratified by cirrhosis and ascites status. Boxplots comparing (A) liver stiffness and (B) median renal R2* values across three patient groups: (I) non-cirrhotic patients; (II) cirrhotic patients without ascites; and (III) cirrhotic patients with ascites. (C,D) Liver stiffness and renal R2* values, respectively, among cirrhotic patients stratified by ascites severity: none, mild, and moderate. Numbers inside boxes indicate median values. MR, magnetic resonance.

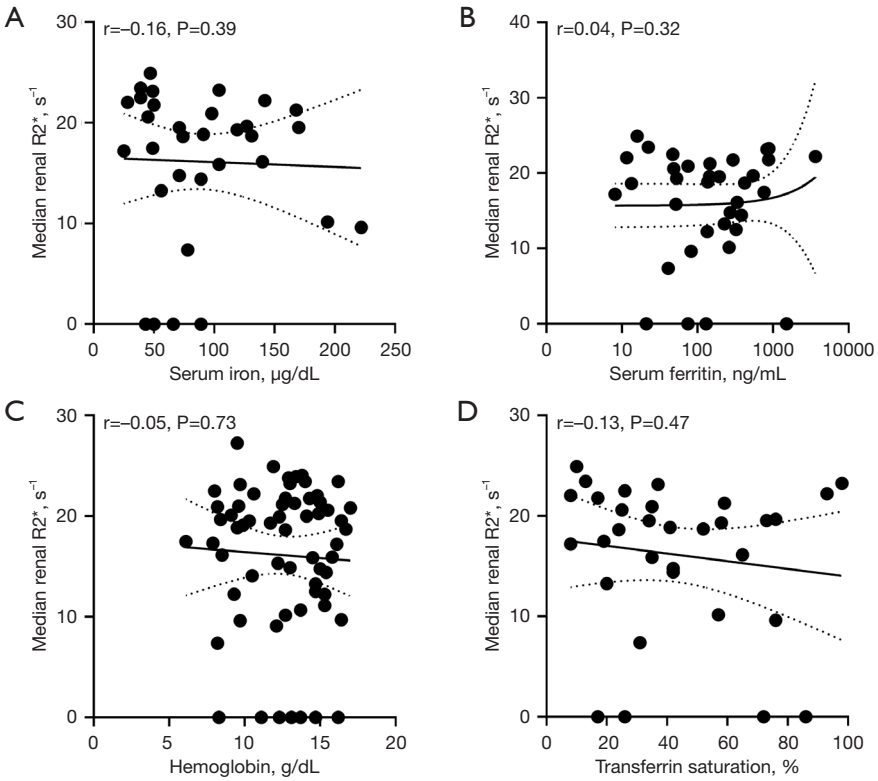

Figure 4 Correlation between median renal R2* values and (A) serum iron, (B) serum ferritin, (C) hemoglobin, and (D) transferrin saturation levels in patients with cirrhosis and ascites.

Correlation between median renal R2 values and iron-related parameters and eGFR*

As shown in *Figure 4*, there were no significant correlations between median renal R2* values and serum iron, ferritin, hemoglobin, and transferrin saturation in patients with cirrhosis and ascites. Furthermore, when this patient group was stratified by iron overload status, no significant difference in median renal R2* values was observed (Figure S2). However, patients who developed HRS-AKD had significantly higher median renal R2* values compared to those who did not (P=0.007). These patients also had lower eGFR values at the time of MRE (59.0 *vs.* 103.6 mL/min/1.73 m^2, P<0.001) (Figure S3). Furthermore, an inverse correlation was identified between median renal R2* values and eGFR measured at MRE (r=–0.34, P=0.006).

Diagnostic accuracy of median renal R2 values, liver stiffness, and serum fibrosis markers for predicting HRS-AKD in cirrhotic patients with ascites*

The ROC curves for differentiating the presence or absence of HRS-AKD based on median renal R2* values, liver stiffness, and serum fibrosis markers in cirrhotic patients with ascites are presented in *Figure 5*. The area under the receiver operating characteristic curve (AUROC) values for diagnosing HRS-AKD using median renal R2* values, APRI, AAR, FIB-4 index, and MRE liver stiffness were 74.5 [95% confidence interval (CI): 57.4–91.6], 52.3 (95% CI: 30.0–74.6), 60.4 (95% CI: 35.0–85.8), 60.2 (95% CI: 36.4–84.0), and 50.3 (95% CI: 28.2–72.5), respectively. Although the median R2* value demonstrated the highest diagnostic accuracy for identifying HRS-AKD, it was not significantly superior to MRE or the serum fibrosis markers (*Table 2*). The optimal cut-off value of median renal R2* was 20.8 s^{-1} with sensitivity of 75.0 (95% CI: 34.9–96.8), and specificity of 74.1 (95% CI: 60.3–85.0).

Multivariable analysis of factors associated with HRS-AKD in cirrhotic patients with ascites

The results of univariable and multivariable analyses identifying independent predictors of HRS-AKD in cirrhotic

patients with ascites are presented in *Table 3*. Among the variables assessed, Child-Pugh score [odds ratio (OR) 1.58; 95% CI: 1.02–2.73; P=0.043], and median renal R2* value ≥20.8 s^{-1} (OR 16.8; 95% CI: 2.50–292.0; P=0.002) were independent predictors of HRS-AKD (*Table 3*). In addition, the incidence of HRS-CKD was significantly higher in patients with a median renal R2* value≥20.8 s^{-1} compared to those with R2* <20.8 s^{-1} (30.0% *vs.* 7.1%, P=0.026; Figure S4).

In a sensitivity analysis stratified by baseline renal function, renal R2* remained independently associated with HRS-AKD (OR 1.35; 95% CI: 1.04–2.18; P=0.012) among patients with preserved baseline renal function (eGFR ≥60 mL/min/1.73 m^2) (Table S1). In contrast, the estimates in the eGFR <60 mL/min/1.73 m^2 subgroup were imprecise due to the limited sample size.

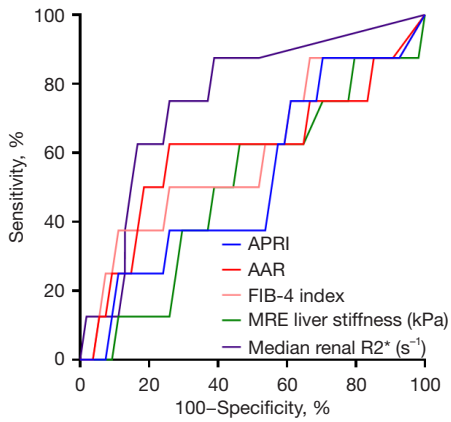

Figure 5 ROC curves demonstrating the diagnostic performance of median renal R2* values, along with liver stiffness and serum fibrosis markers including the AAR, APRI, and FIB-4 index for identifying HRS-AKD in cirrhotic patients with ascites. AAR, aspartate aminotransferase-to-alanine aminotransferase ratio; APRI, aspartate aminotransferase-to-platelet ratio index; FIB-4, fibrosis-4; HRS-AKD, hepatorenal syndrome-acute kidney disease; MRE, magnetic resonance elastography; ROC, receiver operating characteristic.

Discussion

In this study, the median renal R2* value, using an optimal cutoff of 20.8 s^{-1}, was identified as a predictor of HRS-AKD development within 3 months of liver MRE independently of preceding HRS-AKI and Child-Pugh score in patients with cirrhosis and ascites. Renal R2* values did not vary by the amount of ascites and showed no significant correlation with iron-related parameters, including serum iron, ferritin, transferrin saturation and hemoglobin levels. Furthermore, the diagnostic accuracy of median renal R2* for detecting HRS-AKD was higher than that of liver stiffness and serum fibrosis markers. To our knowledge, this is the first study to investigate a potential imaging marker for HRS-AKD and the first to assess a radiologic marker in the context of HRS.

In our study, the incidence of HRS-AKD was 12.9% within patients with cirrhosis and ascites, and reached 31.2% in patients who experienced HRS-AKI, which is comparable to 32% from a previous study (4). Cirrhosis, even in the absence of inherited iron metabolism disorders such as hemochromatosis, can also lead to secondary iron overload due to reduced hepcidin production, resulting in increased intestinal iron absorption and enhanced iron release from macrophages (15,16). Unlike sickle cell disease, in which systemic iron overload arises from intravascular hemolysis and subsequent hemoglobin reabsorption by proximal tubules leads to elevated renal R2* values (17),

Table 2 Diagnostic accuracy of R2* mapping, MRE, and serum fibrosis markers in predicting the development of HRS-AKD in patients with cirrhosis and ascites (n=62)

Variable	Sensitivity	Specificity	PPV	NPV	AUROC	P value	P value (*vs.* R2*)
APRI ≥0.54	87.5 (47.3–99.7)	29.6 (18.0–43.6)	15.6 (6.5–29.5)	94.1 (71.3–99.9)	52.3 (30.0–74.6)	0.84	0.22
AAR ≥2.27	50.0 (15.7–84.3)	74.1 (60.3–85.0)	22.2 (6.4–47.6)	90.9 (78.3–97.5)	60.4 (35.0–85.8)	0.38	0.14
Fibrosis-4 index ≥12.45	37.5 (8.5–75.5)	88.9 (77.4–95.8)	33.3 (7.5–70.1)	90.6 (79.3–96.9)	60.2 (36.4–84.0)	0.38	0.14
MRE liver stiffness ≥5.1 kPa	62.5 (24.5–91.5)	53.7 (39.6–67.4)	16.7 (5.6–34.7)	90.6 (75.0–98.0)	50.3 (28.2–72.5)	0.98	0.24
Median renal R2* ≥20.8 (s^{-1})	75.0 (34.9–96.8)	74.1 (60.3–85.0)	30.0 (11.9–54.3)	95.2 (83.8–99.4)	74.5 (57.4–91.6)	0.011	(Reference)

Data are presented as value (95% CI). AAR, aspartate aminotransferase-to-alanine aminotransferase ratio; APRI, aspartate aminotransferase-to-platelet ratio index; AUROC, area under the receiver operating characteristic curve; CI, confidence interval; HRS-AKD, hepatorenal syndrome-acute kidney disease; MRE, magnetic resonance elastography; NPV, negative predictive value; PPV, positive predictive value; R2*, effective transverse relaxation rate.

Table 3 Univariable and multivariable logistic regression analysis for the development of HRS-AKD in patients with cirrhosis and ascites (n=62)

Variables	Univariable analysis		Multivariable analysis	
	OR (95% CI)	P value	OR (95% CI)	P value
Age (years)	1.05 (0.97–1.14)	0.23		
Sex (male)	0.56 (0.13–2.69)	0.45		
CP score	1.53 (1.07–2.27)	0.019*	1.58 (1.02–2.73)	0.043*
MELD score	1.14 (0.99–1.32)	0.07		
Ascites (moderate *vs.* mild)	1.34 (0.31–5.72)	0.68		
HRS-AKI	5.94 (1.37–29.2)	0.017*	4.83 (0.73–40.0)	0.10
AST (IU/L)	1.00 (0.98–1.02)	0.82		
ALT (IU/L)	0.99 (0.94–1.01)	0.74		
Albumin (g/dL)	0.45 (0.17–1.03)	0.06		
Total bilirubin (mg/dL)	1.07 (0.86–1.26)	0.49		
APRI	1.03 (0.59–1.53)	0.88		
AAR	1.30 (0.83–1.96)	0.23		
Fibrosis-4 index	1.06 (0.94–1.16)	0.32		
MRE (kPa)	0.99 (0.77–1.18)	0.91		
Platelet count (10^3/μL)	0.99 (0.98–1.01)	0.57		
Hemoglobin (g/dL)	0.89 (0.68–1.15)	0.37		
Serum iron (μg/dL)	0.99 (0.96–1.01)	0.17		
Serum ferritin (ng/mL)	1.00 (0.99–1.01)	0.053		
Serum transferrin saturation (%)	0.99 (0.95–1.02)	0.51		
Median renal R2* ≥20.8 (s^{-1})	7.26 (1.64–43.3)	0.009*	16.8 (2.50–292.0)	0.002*

, statistical significance. AAR, aspartate aminotransferase-to-alanine aminotransferase ratio; ALT, alanine aminotransferase; APRI, aspartate aminotransferase-to-platelet ratio index; AST, aspartate aminotransferase; CI, confidence interval; CP, Child-Pugh; HRS-AKD, hepatorenal syndrome-acute kidney disease; HRS-AKI, hepatorenal syndrome acute kidney injury; MELD, Model for End-Stage Liver Disease; MRE, magnetic resonance elastography; OR, odds ratio; R2, effective transverse relaxation rate.

cirrhosis does not involve intravascular hemolysis; therefore, iron overload is unlikely to be the primary contributor to increased renal R2* in our cirrhotic cohort. Consistently, renal R2* values showed no correlation with iron-related parameters and did not differ between patients with and without iron overload. Moreover, although secondary iron overload in cirrhosis has been associated with hepatic decompensation (18), renal R2* values remained similar across varying degrees of ascites.

In addition to serving as a surrogate for tissue iron deposition, several animal and human studies have demonstrated that R2* also reflects renal tissue oxygenation, as it is sensitive to the concentration of paramagnetic deoxyhemoglobin (19-21). In a porcine model, a linear relationship was observed between renal tissue oxygen tension, pO_2, and R2* values in both the cortex and medulla (19). In humans, higher R2* values in patients with CKD have been associated with lower eGFR, indicating reduced renal oxygenation (20). Furthermore, elevated R2* values have been associated with a more rapid decline in kidney function over time (20). Renal R2* measurements have shown good reproducibility, with a coefficient of variation of 4–5% in healthy individuals and approximately 8% in CKD patients over a 1–2 weeks interval (21).

In cirrhosis, splanchnic vasodilatation reduces effective blood volume, triggering the renin-angiotensin-aldosterone system (RAAS), sympathetic activation, and vasopressin release, leading to renal vasoconstriction (5). In severe cases

like HRS, this results in renal hypoxia and acute tubular injury, as confirmed by kidney biopsy findings (22-24). In our study, among cirrhotic patients with ascites, renal R2* values inversely correlated with eGFR measured at the time of MRE and were significantly higher in those who subsequently developed HRS-AKD, suggesting possibly impaired baseline renal oxygenation and function in this subgroup. Importantly, despite its correlation with baseline eGFR, renal R2* remained independently associated with the development of HRS-AKD in sensitivity analyses adjusting for renal function (eGFR ≥60 mL/min/1.73 m^2), supporting the role of renal R2* as a potential early biomarker of renal vulnerability rather than merely a surrogate of established renal dysfunction. In contrast, estimates in patients with baseline eGFR <60 mL/min/1.73 m^2 were imprecise due to limited sample size and should be interpreted with caution. Notably, renal R2* was a better predictor of HRS-AKD development than serum fibrosis markers and MRE liver stiffness, likely because the latter primarily reflect hepatic pathology rather than directly indicating renal dysfunction. Renal R2* also offers advantages over urinary biomarkers for predicting HRS-AKD. Tubular injury markers such as NGAL and IL-18, while useful in detecting HRS-AKI, typically rises within 1 to 12 hours after injury and peak within 12 to 24 hours (9,25), but often decline during the subacute phase, limiting their utility in HRS-AKD. Moreover, their levels can be confounded by urinary tract infections or sepsis (25).

In contrast, renal hypoxia evolves more gradually and may persist into the subacute phase. In a rat model, cortical hypoxia appeared 15 hours after RAAS activation (26), and remained reduced up to two weeks post-injury (27). Additionally, experimental models of CKD have shown that renal hypoxia can precede measurable functional decline (28,29). Additionally, renal hypoxia in cirrhosis may arise not only from intrarenal hemodynamic alterations, but also from systemic metabolic stress-related to hepatic functional compromise (30-32) and inflammation driven by gut-liver interactions (30,33,34). These findings support the role of R2* as a potential imaging marker for predicting HRS-AKD, particularly when urinary biomarkers are less informative. From a clinical perspective, elevated renal R2* values may help identify cirrhotic patients at increased risk of HRS-AKD who could benefit from closer renal surveillance, early optimization of volume status and albumin therapy, and timely referral for transplant evaluation. Furthermore, screening patients who may develop HRS-AKD through R2* may help guide therapeutic interventions, as hypoxia-inducible factor stabilizers such as the anti-anemia agent FG-4592 have demonstrated efficacy in preventing AKI-to-CKD transition in mouse models (35).

There are several limitations to our study. First, it is a retrospective analysis from a single institution, which may introduce selection bias. All cirrhotic patients in this cohort underwent MRE as part of pre-transplant evaluation; therefore, the findings may not be fully generalizable to the broader population of cirrhotic patients who are not transplant candidates. However, multi-echo R2* mapping sequences are widely available and could be integrated into routine liver MRI protocols with minimal additional acquisition time. Therefore, renal R2* assessment may be applied to selected high-risk cirrhotic patients, including those who are not currently transplant candidates. Second, we analyzed R2* values from the left kidney, as it is anatomically positioned higher than the right, and in most cases, MRE did not provide full coverage of the right kidney, limiting the reliability of quantitative analysis. Although R2* mapping is not routinely performed for the kidneys in clinical practice and is not part of standard dynamic renal MRI protocols, future studies dedicated to renal R2* mapping are warranted to assess the reproducibility and reliability of bilateral renal R2* measurements. Third, the renal medulla is known to be more susceptible to hypoxic injury than the cortex, with higher R2* values reported in patients with diabetic nephropathy (36). However, there are no distinct anatomic landmarks separating the cortex and medulla, and these regions cannot be reliably distinguished on R2* maps. Therefore, renal quantification could not be performed separately for the cortex and medulla. Fourth, renal biopsy data were not available to confirm R2* as a direct surrogate for hypoxia or tubular injury, as biopsy is not routinely performed in patients undergoing MRE. Lastly, we did not compare R2* values with urinary biomarkers, as no established urinary marker exists for HRS-AKD, and tests such as NGAL and IL-18 were not routinely performed. In addition, only a small number of HRS-AKD events occurred in our cohort, and therefore the multivariable analysis should be considered exploratory. Although we applied penalized regression to reduce small-sample bias, the estimates should be interpreted with caution, and validation in larger, prospective cohort is warranted.

Conclusions

In conclusion, renal R2* appears to be a promising

noninvasive imaging marker for predicting the development of HRS-AKD in cirrhotic patients with ascites, and may aid in identifying those at risk for AKI-to-CKD transition.

Acknowledgments

None.

Footnote

Reporting Checklist: The authors have completed the STROBE reporting checklist. Available at https://qims.amegroups.com/article/view/10.21037/qims-2025-aw-2262/rc

Data Sharing Statement: Available at https://qims.amegroups.com/article/view/10.21037/qims-2025-aw-2262/dss

Funding: This study was supported by Yonsei Institute for Digital Health Fund (No. 6-2025-0113).

Conflicts of Interest: All authors have completed the ICMJE uniform disclosure form (available at https://qims.amegroups.com/article/view/10.21037/qims-2025-aw-2262/coif). The authors have no conflicts of interest to declare.

Ethical Statement: The authors are accountable for all aspects of the work in ensuring that questions related to the accuracy or integrity of any part of the work are appropriately investigated and resolved. The study was conducted in accordance with the Declaration of Helsinki and its subsequent amendments. The study was approved by Institutional Review Board (IRB) of Severance Hospital, Seoul, Korea (IRB No. 2025-0959-001) and individual consent for this retrospective analysis was waived.

References

1. Nadim MK, Kellum JA, Forni L, Francoz C, Asrani SK, Ostermann M, et al. Acute kidney injury in patients with cirrhosis: Acute Disease Quality Initiative (ADQI) and International Club of Ascites (ICA) joint multidisciplinary consensus meeting. J Hepatol 2024;81:163-83.
2. Tonon M, Rosi S, Gambino CG, Piano S, Calvino V, Romano A, Martini A, Pontisso P, Angeli P. Natural history of acute kidney disease in patients with cirrhosis. J Hepatol 2021;74:578-83.
3. Bassegoda O, Huelin P, Ariza X, Solé C, Juanola A, Gratacós-Ginès J, Carol M, Graupera I, Pose E, Napoleone L, Albertos S, de Prada G, Cervera M, Fernández J, Fabrellas N, Poch E, Solà E, Ginès P. Development of chronic kidney disease after acute kidney injury in patients with cirrhosis is common and impairs clinical outcomes. J Hepatol 2020;72:1132-9.
4. Patidar KR, Naved MA, Grama A, Adibuzzaman M, Aziz Ali A, Slaven JE, Desai AP, Ghabril MS, Nephew L, Chalasani N, Orman ES. Acute kidney disease is common and associated with poor outcomes in patients with cirrhosis and acute kidney injury. J Hepatol 2022;77:108-15.
5. Erly B, Carey WD, Kapoor B, McKinney JM, Tam M, Wang W. Hepatorenal Syndrome: A Review of Pathophysiology and Current Treatment Options. Semin Intervent Radiol 2015;32:445-54.
6. Salerno F, Gerbes A, Ginès P, Wong F, Arroyo V. Diagnosis, prevention and treatment of hepatorenal syndrome in cirrhosis. Gut 2007;56:1310-8.
7. Angeli P, Garcia-Tsao G, Nadim MK, Parikh CR. News in pathophysiology, definition and classification of hepatorenal syndrome: A step beyond the International Club of Ascites (ICA) consensus document. J Hepatol 2019;71:811-22.
8. Puthumana J, Ariza X, Belcher JM, Graupera I, Ginès P, Parikh CR. Urine Interleukin 18 and Lipocalin 2 Are Biomarkers of Acute Tubular Necrosis in Patients With Cirrhosis: A Systematic Review and Meta-analysis. Clin Gastroenterol Hepatol 2017;15:1003-1013.e3.
9. Allegretti AS, Solà E, Ginès P. Clinical Application of Kidney Biomarkers in Cirrhosis. Am J Kidney Dis 2020;76:710-9.
10. Jo SK, Yang J, Hwang SM, Lee MS, Park SH. Role of biomarkers as predictors of acute kidney injury and mortality in decompensated cirrhosis. Sci Rep 2019;9:14508.
11. Simonetto DA, Gines P, Kamath PS. Hepatorenal

syndrome: pathophysiology, diagnosis, and management. BMJ 2020;370:m2687.
12. Aithal GP, Palaniyappan N, China L, Härmälä S, Macken L, Ryan JM, Wilkes EA, Moore K, Leithead JA, Hayes PC, O'Brien AJ, Verma S. Guidelines on the management of ascites in cirrhosis. Gut 2021;70:9-29.
13. EASL Clinical Practice Guidelines for the management of patients with decompensated cirrhosis. J Hepatol 2018;69:406-60.
14. Kowdley KV. Iron Overload in Patients With Chronic Liver Disease. Gastroenterol Hepatol (N Y) 2016;12:695-8.
15. Girelli D, Pasino M, Goodnough JB, Nemeth E, Guido M, Castagna A, Busti F, Campostrini N, Martinelli N, Vantini I, Corrocher R, Ganz T, Fattovich G. Reduced serum hepcidin levels in patients with chronic hepatitis C. J Hepatol 2009;51:845-52.
16. Abu Rajab M, Guerin L, Lee P, Brown KE. Iron overload secondary to cirrhosis: a mimic of hereditary haemochromatosis? Histopathology 2014;65:561-9.
17. Aslan E, Luo JW, Lesage A, Paquin P, Cerny M, Chin AS, Olivié D, Gilbert G, Soulières D, Tang A. MRI-based R2* mapping in patients with suspected or known iron overload. Abdom Radiol (NY) 2021;46:2505-15.
18. Kayali Z, Ranguelov R, Mitros F, Shufelt C, Elmi F, Rayhill SC, Schmidt WN, Brown KE. Hemosiderosis is associated with accelerated decompensation and decreased survival in patients with cirrhosis. Liver Int 2005;25:41-8.
19. Pedersen M, Dissing TH, Mørkenborg J, Stødkilde-Jørgensen H, Hansen LH, Pedersen LB, Grenier N, Frøkiaer J. Validation of quantitative BOLD MRI measurements in kidney: application to unilateral ureteral obstruction. Kidney Int 2005;67:2305-12.
20. Pruijm M, Mendichovszky IA, Liss P, Van der Niepen P, Textor SC, Lerman LO, Krediet CTP, Caroli A, Burnier M, Prasad PV. Renal blood oxygenation level-dependent magnetic resonance imaging to measure renal tissue oxygenation: a statement paper and systematic review. Nephrol Dial Transplant 2018;33:ii22-8.
21. Khatir DS, Pedersen M, Jespersen B, Buus NH. Reproducibility of MRI renal artery blood flow and BOLD measurements in patients with chronic kidney disease and healthy controls. J Magn Reson Imaging 2014;40:1091-8.
22. Arroyo V, Angeli P, Moreau R, Jalan R, Clària J, Trebicka J, Fernández J, Gustot T, Caraceni P, Bernardi M; investigators from the EASL-CLIF Consortium, Grifols Chair and European Foundation for the Study of Chronic Liver Failure (EF-Clif). The systemic inflammation hypothesis: Towards a new paradigm of acute decompensation and multiorgan failure in cirrhosis. J Hepatol 2021;74:670-85.
23. Mandal AK, Lansing M, Fahmy A. Acute tubular necrosis in hepatorenal syndrome: an electron microscopy study. Am J Kidney Dis 1982;2:363-74.
24. Trawalé JM, Paradis V, Rautou PE, Francoz C, Escolano S, Sallée M, Durand F, Valla D, Lebrec D, Moreau R. The spectrum of renal lesions in patients with cirrhosis: a clinicopathological study. Liver Int 2010;30:725-32.
25. Liu Y, Li C, Yang X, Guo S, Cui Z, Kang H, Ma Z, Wang H. Neutrophil Gelatinase-Associated Lipocalin and Interleukin-18 in the Prediction of Acute Kidney Injury in Sepsis Patients. Int J Gen Med 2024;17:6335-41.
26. Emans TW, Janssen BJ, Pinkham MI, Ow CP, Evans RG, Joles JA, Malpas SC, Krediet CT, Koeners MP. Exogenous and endogenous angiotensin-II decrease renal cortical oxygen tension in conscious rats by limiting renal blood flow. J Physiol 2016;594:6287-300.
27. Papazova DA, Friederich-Persson M, Joles JA, Verhaar MC. Renal transplantation induces mitochondrial uncoupling, increased kidney oxygen consumption, and decreased kidney oxygen tension. Am J Physiol Renal Physiol 2015;308:F22-8.
28. dos Santos EA, Li LP, Ji L, Prasad PV. Early changes with diabetes in renal medullary hemodynamics as evaluated by fiberoptic probes and BOLD magnetic resonance imaging. Invest Radiol 2007;42:157-62.
29. Manotham K, Tanaka T, Matsumoto M, Ohse T, Miyata T, Inagi R, Kurokawa K, Fujita T, Nangaku M. Evidence of tubular hypoxia in the early phase in the remnant kidney model. J Am Soc Nephrol 2004;15:1277-88.
30. Adebayo D, Wong F. Pathophysiology of Hepatorenal Syndrome - Acute Kidney Injury. Clin Gastroenterol Hepatol 2023;21:S1-S10.
31. Mindikoglu AL, Opekun AR, Putluri N, Devaraj S, Sheikh-Hamad D, Vierling JM, et al. Unique metabolomic signature associated with hepatorenal dysfunction and mortality in cirrhosis. Transl Res 2018;195:25-47.
32. Lee JZ, Ng SJKK, Shelat VG. Metabolic changes after hepatectomy: Implications for perioperative management and long-term outcomes. World J Gastrointest Pathophysiol 2025;16:109860.
33. Shah N, Mohamed FE, Jover-Cobos M, Macnaughtan J, Davies N, Moreau R, Paradis V, Moore K, Mookerjee R, Jalan R. Increased renal expression and urinary excretion of TLR4 in acute kidney injury associated with cirrhosis. Liver Int 2013;33:398-409.
34. Wang JDJ, Suan E, Li SS, Shelat VG. Sepsis and the

diverse organ-gastrointestinal tract axis. World J Crit Care Med 2025;14:105547.
35. Wu M, Chen W, Miao M, Jin Q, Zhang S, Bai M, Fan J, Zhang Y, Zhang A, Jia Z, Huang S. Anti-anemia drug FG4592 retards the AKI-to-CKD transition by improving vascular regeneration and antioxidative capability. Clin Sci (Lond) 2021;135:1707-26.
36. Liu J, Yang D, Tian C, Lv R, Wang R, Zeng X. Magnetic resonance imaging for noninvasive assessment of renal fat deposition and hypoxia in diabetic kidney disease. BMC Med Imaging 2025;25:272.

Cite this article as: Park JH, Park HJ, Choi D, Yoon J. Renal R2* as a noninvasive predictor of hepatorenal syndrome-acute kidney disease in cirrhotic patients with ascites: a retrospective cohort study. Quant Imaging Med Surg 2026;16(6):463. doi: 10.21037/qims-2025-aw-2262

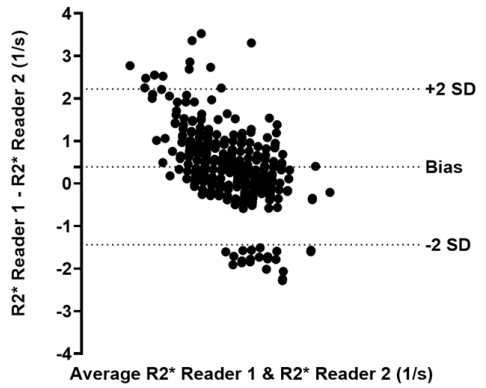

Figure S1 Bland-Altman plot showing inter-reader agreement for median renal R2* measurements.

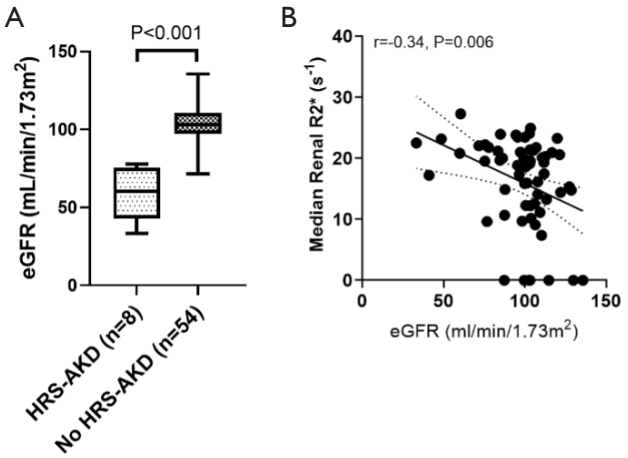

Figure S3 Association between renal function and renal R2* in cirrhotic patients with ascites. (A) Comparison of eGFR between cirrhotic patients with ascites who developed HRS-AKD and those who did not. (B) Correlation between median renal R2* values and eGFR measured at MRE in cirrhotic patients with ascites. eGFR, estimated glomerular filtration rate; HRS-AKD, hepatorenal syndrome-acute kidney disease; MRE, magnetic resonance elastography.

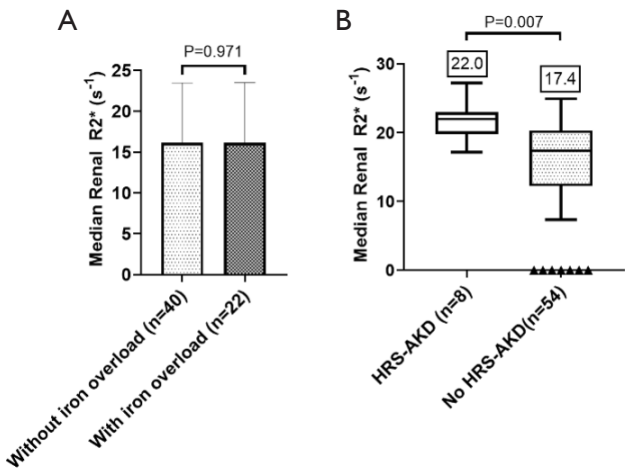

Figure S2 Association of renal R2* with iron overload and HRS-AKD in cirrhotic patients with ascites. (A) Comparison of median renal R2* values between cirrhotic patients with ascites with and without iron overload. (B) Comparison of median renal R2* values between cirrhotic patients with ascites who developed HRS-AKD and those who did not. HRS-AKD, hepatorenal syndrome-acute kidney disease.

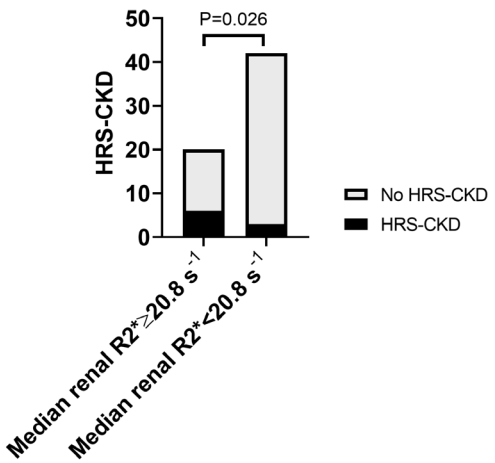

Figure S4 Incidence of HRS-CKD in cirrhotic patients with ascites stratified by median renal R2* values ≥20.8 and <20.8. HRS-CKD, hepatorenal syndrome-chronic kidney disease.

https://dx.doi.org/10.21037/qims-2025-aw-2262

Table S1 Sensitivity analysis stratified by baseline eGFR in patients with cirrhosis and ascites (n=62)

Variables	eGFR ≥60 mL/min/1.73m^2 (n=56)		eGFR <60 mL/min/1.73m^2 (n=6)	
	OR (95% CI)	P value	OR (95% CI)	P value
CP score	1.67 (0.98-3.36)	0.06	1.15 (0.01-205.67)	0.93
HRS-AKI	2.76 (0.28-22.05)	0.35	0.79 (0.00-1064.9)	0.96
Median renal R2* ≥20.8 s^{-1}	1.35 (1.04-2.18)	0.012*	1.03 (0.08-4.34)	0.95

, statistical significance. CI, confidence interval; CP, Child-Pugh; eGFR, estimated glomerular filtration rate; HRS-AKD, hepatorenal syndrome-acute kidney disease; OR, odds ratio; R2, effective transverse relaxation rate.

https://dx.doi.org/10.21037/qims-2025-aw-2262